INTERNATIONAL JOURNAL FOR NUMERICAL METHODS IN FLUIDS
Int. J. Numer. Meth. Fluids 2003; **42**:1345–1361 (DOI: 10.1002/fld.593)

Detecting instabilities in flows of viscoelastic fluids

N. Fiétier*,†

Laboratory of Computational Engineering, School of Engineering, Ecole Polytechnique Fédérale de Lausanne, CH-1015 Lausanne, Switzerland

SUMMARY

There is a growing interest in developing numerical tools to investigate the onset of physical instabilities observed in experiments involving viscoelastic flows, which is a difficult and challenging task as the simulations are very sensitive to numerical instabilities. Following a recent linear stability analysis carried out in order to better understand qualitatively the origin of numerical instabilities occurring in the simulation of flows viscoelastic fluids, the present paper considers a possible extension for more complex flows. This promising method could be applied to track instabilities in complex (i.e. essentially non-parallel) flows. In addition, results related to transient growth mechanism indicate that it might be responsible for the development of numerical instabilities in the simulation of viscoelastic fluids.

KEY WORDS: instabilities; stability analysis; viscoelastic fluids; Arnoldi method; transient growth

1. INTRODUCTION

The maximum processing rate that can be obtained in typical polymer processing operations is often limited by the occurrence of elastic instabilities, which are not present in the corresponding flow of Newtonian fluids. It is therefore interesting to understand the driving mechanisms and to determine both spatial and temporal characteristics of these instabilities. To do so, their onsets in a number of special test benchmarks that model individual elements of complex industrial processing geometries have been studied and well documented [1–6]. In the past decade, rather extensive research work has been carried out in order to come to a better understanding of the mechanism driving the inception of instabilities. The most successful investigations have been achieved so far with experiments although significant progress has also been reported with theoretical stability analyses. Detecting such instabilities

*Correspondence to: N. Fiétier, Laboratory of Computational Engineering, Swiss Federal Institute of Technology–Lausanne, CH-1015 Lausanne, Switzerland.
†E-mail: Nicolas.Fietier@epfl.ch

Contract/grant sponsor: Swiss National Science Foundation; contract/grant number: 20-S9357599

Received 19 December 2002
Revised 29 April 2003

with large computational simulations remains a very difficult and challenging task even with today's computer resources [7].

Stability analyses are very often conducted in order to establish if a steady solution can be maintained with superposed perturbations. Analytical methods used for stability analysis are described in numerous textbooks [8–11]. Three types of analysis are usually performed. They are, respectively, aimed at determining conditions under which a process is absolutely unstable no matter what perturbation amplitude is selected (non-linear stability analysis), evaluating the effect of a small-amplitude perturbation when approaching the conditions of an absolute instability (linear stability analysis) and establishing the conditions of absolute stability without considering the perturbation amplitude. Either the stability of the constitutive equation itself e.g. References [12, 13] or the influence of the discretization method on the stability [14–16] can be studied.

In classical linear stability, analyses aimed at determining the inherent stability properties of constitutive equations, specific Fourier expansions of the perturbations in the streamwise direction are considered e.g. References [12, 17]. This results in solving eigenvalue spectra with rather large number of Chebyshev polynomials (typically 100). A complementary analysis proposed recently [15, 16] has been carried out in order to better understand qualitatively the origin of numerical instabilities occurring in the simulation of the flows viscoelastic fluids [16, 18]. It focussed on computing the eigenvalue spectra generated by the discretization itself. Only spatial discretizations with a limited number of grid points or polynomial order corresponding to the values used for the simulation of complex problems with the spectral elements were considered in the corresponding study. The present paper considers a possible extension of this linear stability analysis for more complex flows since no explicit construction of matrices occurring in the resulting generalized eigenvalue problem is required. Numerical investigation of the stability of complex viscoelastic flows is an emerging domain of research e.g. References [7, 19]. Techniques based on implicitly restarted Arnoldi methods (IRAM) [20, 21] enabling a certain number of leading eigenvalues to be determined have been proposed to investigate the stability of complex flows e.g. References [7, 22]. We present in Section 3 an implementation of such a technique.

Transient growth is sometimes attributed to the existence of degenerate or nearly degenerate eigenvalues of the linearized stability problem. Non-normality associated to the non-commutability with its adjoint of the linearized differential operator can be held responsible for the linear growth of perturbations, which may lead to the transition from laminar to turbulent flow for Newtonian fluids [23, 24] or to transient phenomena in viscoelastic flows e.g. [19, 25]. Transient growth can also be associated with the development of numerical instabilities during transient viscoelastic flow simulations [14, 15] as described in Section 4.

As noticed, most, if not all, numerical investigations of instabilities developing in complex (i.e. essentially non-parallel) flows of viscoelastic fluids have been carried out with low-order finite element or volume methods. High-order accurate methods possessing suitable properties of low dispersion and diffusion are certainly potentially relevant candidates to accomplish such studies as shown for Newtonian flows e.g. by Leriche [26] with a spectral Chebyshev-tau method for a three-dimensional (3D) lid-driven cavity or Fischer [27, 28] with conforming and non-conforming Legendre spectral element methods for various complex time-dependent problems. The feasibility of using spectral element methods to simulate viscoelastic flows has been demonstrated by several authors e.g. References [18, 29, 30]. We have considered such a method for the spatial discretization of the problems discussed in this paper.

The paper is organized as follows. The basic and linearized equations leading to the derivation of a generalized eigenvalue problem are introduced in Section 2. After presenting in Section 3.1 the Arnoldi-based computational method enabling us to determine specific eigenvalues and proceed to linear stability analysis of flows without drastic restriction on mesh size, we discuss results obtained with such analyses in Section 3.2. Possible applications to complex flows are described in Section 3.3. Some study of the transient growth mechanism is reported in Section 4.

2. LINEARIZATION OF THE FLOW EQUATIONS

In this section, we present the conservation and constitutive equations in non-dimensional form, derive the related linearized equations and express the corresponding generalized eigenvalue problem for flows of Oldroyd-B fluids as an example. The methodology can be readily applied to any type of viscoelastic fluid with a constitutive equation written in differential form. Other examples can be obtained in Reference [16].

Let us recall that the set of equations associated with the Oldroyd-B model in non-dimensional form

$$\nabla \cdot \mathbf{v} = 0 \tag{1}$$

$$\frac{\partial \mathbf{v}}{\partial t} = -Re(\mathbf{v} \cdot \nabla)\mathbf{v} - \nabla p + R_\mu \nabla^2 \mathbf{v} + \nabla \cdot \boldsymbol{\tau} \tag{2}$$

$$We\left[\frac{1}{Re}\frac{\partial \boldsymbol{\tau}}{\partial t} + (\mathbf{v} \cdot \nabla)\boldsymbol{\tau} - \boldsymbol{\tau} \cdot (\nabla \mathbf{v})^{\mathrm{T}} - \nabla \mathbf{v} \cdot \boldsymbol{\tau}\right] + \boldsymbol{\tau} = 2(1 - R_\mu)\mathbf{D} \tag{3}$$

In the previous equations, the velocity $\mathbf{v}$, co-ordinates $\mathbf{x}$, viscoelastic stress $\boldsymbol{\tau}$, pressure p and time t are, respectively, scaled with the following quantities: V (reference velocity), L_{r} (reference length), $S = \mu_{\mathrm{t}} V/L_{\mathrm{r}}$, $P = S$, $T = \rho L_{\mathrm{r}}^2/\mu_{\mathrm{t}}$, where ρ and μ_{t} are the fluid density and (total) viscosity. The quantity $R_\mu = \mu_{\mathrm{s}}/\mu_{\mathrm{t}}$ is the ratio of the solvent viscosity over the total viscosity. The non-dimensional numbers $Re = \rho V L_{\mathrm{r}}/\mu_{\mathrm{t}}$ and $We = \lambda V/L_{\mathrm{r}}$ are, respectively, the Reynolds and Weissenberg numbers where λ is the relaxation time of the viscoelastic fluid.

In order to perform this analysis, the set of equations (1)–(3) is linearized by looking for a solution composed of a perturbation $(p_1, \mathbf{v}_1, \boldsymbol{\tau}_1)$ added to a known solution of the system of equation $(p_0, \mathbf{v}_0, \boldsymbol{\tau}_0)$ (steady 2D base flow):

$$p = p_0 + p_1, \quad \mathbf{v} = \mathbf{v}_0 + \mathbf{v}_1, \quad \boldsymbol{\tau} = \boldsymbol{\tau}_0 + \boldsymbol{\tau}_1 \tag{4}$$

which induces the following set of equations if the first-order perturbation terms are retained:

$$\nabla \cdot \mathbf{v}_1 = 0 \tag{5}$$

$$\frac{\partial \mathbf{v}_1}{\partial t} = -Re[(\mathbf{v}_0 \cdot \nabla)\mathbf{v}_1 + (\mathbf{v}_1 \cdot \nabla)\mathbf{v}_0] - \nabla p_1 + R_\mu \nabla^2 \mathbf{v}_1 + \nabla \cdot \boldsymbol{\tau}_1 \tag{6}$$

$$-2(1 - R_\mu)\mathbf{D}(\mathbf{v}_1) + \boldsymbol{\tau}_1 + We\left[\frac{1}{Re}\frac{\partial \boldsymbol{\tau}_1}{\partial t} + (\mathbf{v}_0 \cdot \nabla)\boldsymbol{\tau}_1 + (\mathbf{v}_1 \cdot \nabla)\boldsymbol{\tau}_0\right]$$
$$-We[\boldsymbol{\tau}_1 \cdot (\nabla \mathbf{v}_0)^{\mathrm{T}} - \nabla \mathbf{v}_0 \cdot \boldsymbol{\tau}_1 - \boldsymbol{\tau}_0 \cdot (\nabla \mathbf{v}_1)^{\mathrm{T}} - \nabla \mathbf{v}_1 \cdot \boldsymbol{\tau}_0] = 0 \tag{7}$$

where

$$\mathbf{D}(\mathbf{v}_1) = \tfrac{1}{2}(\nabla \mathbf{v}_1 + (\nabla \mathbf{v}_1)^{\mathrm{T}}) \tag{8}$$

Introducing a perturbation of the type

$$(p_1 = P_1 \mathrm{e}^{vt}, \mathbf{v}_1 = \mathbf{V}_1 \mathrm{e}^{vt}, \boldsymbol{\tau}_1 = \mathbf{T}_1 \mathrm{e}^{vt}) \tag{9}$$

leads to the following set of equations:

$$\nabla \cdot \mathbf{V}_1 = 0 \tag{10}$$

$$v\mathbf{V}_1 = -\nabla P_1 + R_\mu \nabla^2 \mathbf{V}_1 - C(\mathbf{v}_0, \mathbf{V}_1) + \nabla \cdot \mathbf{T}_1 \tag{11}$$

$$v \frac{We}{Re} \mathbf{T}_1 = -\mathbf{T}_1 - NL_T(\mathbf{v}_0, \boldsymbol{\tau}_0, \mathbf{T}_1) - NL_V(\boldsymbol{\tau}_0, \mathbf{V}_1) \tag{12}$$

where

$$C(\mathbf{v}_0, \mathbf{V}_1) = Re[(\mathbf{v}_0 \cdot \nabla)\mathbf{V}_1 + (\mathbf{V}_1 \cdot \nabla)\mathbf{v}_0] \tag{13}$$

$$NL_T(\mathbf{v}_0, \mathbf{T}_1) = We[(\mathbf{v}_0 \cdot \nabla)\mathbf{T}_1 - \mathbf{T}_1 \cdot (\nabla \mathbf{v}_0)^{\mathrm{T}} - \nabla \mathbf{v}_0 \cdot \mathbf{T}_1] \tag{14}$$

$$NL_V(\boldsymbol{\tau}_0, \mathbf{V}_1) = We[(\mathbf{V}_1 \cdot \nabla)\boldsymbol{\tau}_0 - \boldsymbol{\tau}_0 \cdot (\nabla \mathbf{V}_1)^{\mathrm{T}} - \nabla \mathbf{V}_1 \cdot \boldsymbol{\tau}_0] - 2(1 - R_\mu)\mathbf{D}(\mathbf{V}_1) \tag{15}$$

which can be written in operator-matrix form

$$vBx = Ax \tag{16}$$

where $x^{\mathrm{T}} = [P_1, \mathbf{V}_1, \mathbf{T}_1]^{\mathrm{T}}$:

$$\begin{aligned} v \begin{bmatrix} 0 & 0 & 0 \\ 0 & (\mathbf{I}) & 0 \\ 0 & 0 & \dfrac{We}{Re}(\mathbf{I}) \end{bmatrix} \begin{bmatrix} P_1 \\ \mathbf{V}_1 \\ \mathbf{T}_1 \end{bmatrix} \\ = \begin{bmatrix} 0 & \nabla \cdot (\mathbf{I}) & 0 \\ -\nabla(\mathbf{I}) & -C(\mathbf{v}_0, \mathbf{I}) + R_\mu \nabla^2(\mathbf{I}) & \nabla \cdot (\mathbf{I}) \\ 0 & -NL_V(\boldsymbol{\tau}_0, \mathbf{I}) & -(\mathbf{I}) - NL_T(\mathbf{v}_0, \mathbf{I}) \end{bmatrix} \begin{bmatrix} P_1 \\ \mathbf{V}_1 \\ \mathbf{T}_1 \end{bmatrix} \end{aligned} \tag{17}$$

where $(\mathbf{I})$ represents the identity operator. Introducing the spectral element spatial discretization at this stage after expressing previous equations in weak form, leads to the generalized eigenvalue problem

$$vB_h \underline{X} = A_h \underline{X} \tag{18}$$

i.e. explicitly

$$v\begin{bmatrix}0 & 0 & 0\\ 0 & M & 0\\ 0 & 0 & \dfrac{We}{Re}M\end{bmatrix}\begin{bmatrix}\underline{P}\\ \underline{V}\\ \underline{T}\end{bmatrix}=\begin{bmatrix}0 & D & 0\\ D^{\mathrm{T}} & K & A_{VT}\\ 0 & A_{TV} & A_{TT}\end{bmatrix}\begin{bmatrix}\underline{P}\\ \underline{V}\\ \underline{T}\end{bmatrix} \tag{19}$$

where $\underline{P}$, $\underline{V}$ and $\underline{T}$, respectively, represent the vectors associated with the degrees of freedom at the pressure nodes, the two components of the velocity and the three components of the symmetric viscoelastic stress tensor. The matrix M is the mass matrix. The matrices D, D^{T}, K result, respectively, from the discretization of the velocity divergence in the continuity equation, pressure gradient and Laplacian. The matrices A_{VT}, A_{TV} and A_{TT} correspond, respectively, to the discretization of the viscoelastic stress divergence in the momentum equation, velocity and viscoelastic stress operators NL_V and NL_T in the constitutive equation.

3. INVESTIGATING THE STABILITY OF FLOWS

3.1. Computational method

The previous problem can be solved in order to perform a linear stability analysis of the viscoelastic flow. In particular, the influence of the discretization method on the stability can be investigated [15, 16]. For complex flows, it is not affordable to build explicitly the matrices of the eigenvalue problems and use a classical QZ algorithm to solve the entire spectrum as this can be done for simple flows [15, 16]. Leading eigenvalues can be computed via an Arnoldi method applied to a modified eigenvalue problem [31] as shown below. No explicit construction of matrices is required by this method, since only matrix–vector multiplications are involved as emphasized by Tuckerman *et al.* e.g. References [32, 33]. It is thus possible to take advantage of the efficiency of the tensor-product factorization involved in the spectral element method. Using such a method for linear stability analysis with the aim of validating the physical onset of an instability during simulations is a complementary technique to direct simulations. It also enables the invariance of the instability characteristics (in particular the corresponding frequencies) with mesh refinement to be checked.

We will briefly present the basic concept of Arnoldi's method e.g. Reference [31]. As shown in Section 2, the linear stability problem can be reduced to a generalized eigenvalue problem of the type: $v\mathbf{B}X=\mathbf{A}X$, which in turn can be reduced to the simple eigenproblem $\mathbf{C}X=\omega X$ by using a shift-and-invert technique so that $\mathbf{C}\equiv(\mathbf{A}-v_s\mathbf{B})^{-1}\mathbf{B}$ and $\omega=1/(v-v_s)$ where v_s is a relevant real or complex number chosen to eliminate dominant eigenvalues of the generalized eigenvalue problem with very large moduli and to determine eigenvalues located in the vicinity of v_s.

Eigenvectors X are approximated by their projection $X^{(m)}$ onto a set of m orthonormal basis vectors V_i ($m \ll \dim(X)$):

$$X^{(m)}=\sum_{i=1}^{m}\tilde{x}_i^{(m)}V_i \tag{20}$$

The coefficients $\tilde{x}_i^{(m)}$ are determined by imposing that

$$V_j^{\mathrm{T}} \cdot (\mathbf{C}X^{(m)} - \tilde{\omega}^{(m)}X^{(m)}) = 0, \quad j = 1, \ldots, m \tag{21}$$

where $\tilde{\omega}^{(m)}$ is an approximation of an eigenvalue ω of $\mathbf{C}$. The last equation can be written in matrix form

$$[(\mathbf{V}^{(m)})^{\mathrm{T}}\mathbf{C}\mathbf{V}^{(m)} - \tilde{\omega}^{(m)}(\mathbf{V}^{(m)})^{\mathrm{T}}\mathbf{V}^{(m)}]\tilde{X}^{(m)} = 0 \tag{22}$$

where the matrix $\mathbf{V}^{(m)}$ is built by taking its columns identical to the m vectors V_i. The components of the vector $\tilde{X}^{(m)}$ are the coefficients $\tilde{x}_i^{(m)}$. The $m \times m$ matrix $(\mathbf{V}^{(m)})^{\mathrm{T}}\mathbf{C}\mathbf{V}^{(m)}$ is denoted by $\mathbf{H}^{(m)}$.

The vectors V_l are determined by the following sequence:

$$\hat{V}_{l+1} = \mathbf{C}V_l - \sum_{k=1}^{l} (V_k^{\mathrm{T}}\mathbf{C}V_l)V_k \tag{23}$$

$$V_{l+1} = \frac{\hat{V}_{l+1}}{\sqrt{\hat{V}_{l+1}^{\mathrm{T}} \cdot \hat{V}_{l+1}}} \tag{24}$$

An estimate of the norm of the residual corresponding to the jth eigenvalue is obtained by

$$\mathrm{Res}_j = \|\mathbf{C}X_j^{(m)} - \tilde{\omega}_j^{(m)}X_j^{(m)}\| = \sqrt{\hat{V}_{m+1}^{\mathrm{T}} \cdot \hat{V}_{m+1}}\,|E_m^{\mathrm{T}}\tilde{X}_j^{(m)}| \tag{25}$$

where E_m^{T} is a vector of dimension m such that

$$E_m^{\mathrm{T}} = (0, 0, \ldots, 0, 1) \tag{26}$$

This algorithm is used until the residual norm for each eigenvalue is lower than a predefined threshold.

To summarize, Arnoldi's method consists of building an orthogonal system from the Krylov vectors $V_1, \mathbf{C}V_1, \ldots, \mathbf{C}^{m-1}V_1$ with a chosen vector V_1 of unit Euclidian norm. It enables approximations $(\mathbf{V}^{(m)}X_{\mathbf{H}}^{(j)}, \tilde{\omega}_{(j)})$ $(1 \leqslant j \leqslant m)$ of some eigenpairs of the matrix $\mathbf{C}$ to be obtained, where $X_{\mathbf{H}}^{(j)}$ is an eigenvector of $\mathbf{H}^{(m)}$. The matrix $\mathbf{H}^{(m)}$ can be easily diagonalized e.g. by using a QR algorithm.

If applied as described above, the orthonormalization process may become polluted by cancellation errors and more sophisticated techniques like the modified Gram–Schmidt reorthogonalization procedures have been recommended [34]. Accordingly, we have used the IRAM subroutine *dnaupd* of the ARPACK library [21] in our computational code. This technique allows the often excessive requirements of the original algorithm presented before to be overcome, from both storage and computational points of view. It combines the so-called implicitly shifted QR scheme with a k-step Arnoldi factorization to obtain a truncated form of the implicitly shifted QR-iteration [21]. Although the option of explicitly building the matrix $\mathbf{C}$ for problems of small sizes has been retained, we have taken advantage of the genuine ability of the spectral element method to compute matrix–vector products without explicit matrix formulation. This subroutine has been used successfully for solving eigenvalues of the simple Couette and Poiseuille benchmark problems as shown in Section 3.2.

As presented in Section 2 (cf. Equations (5)–(7)), the set of linearized conservation and constitutive equations can be expressed with a formal equation of the type

$$\mathscr{B}\frac{\partial X}{\partial t} = \mathscr{A}X \tag{27}$$

where $X^{\mathrm{T}} = (p, \mathbf{v}, \tau)$ and $\mathscr{A}$ and $\mathscr{B}$ are two operators. After discretizing in space, one obtains the equation relative to the semi-discrete problem Equation (16). Applying a time discretization procedure in addition to the space discretization may be formally described by an operator C_T defined by

$$X^{n+1} = X((n+1)\Delta t) = C_T X^n \tag{28}$$

where X^n is the vector of all degrees of freedom at time step n. Applying this operator is nothing but computing a time step when proceeding to numerical simulations. For instance, using the combination of backward difference formula (BDF) and extrapolation (EX) schemes for implicit linear (e.g. pressure and viscous) and explicit (e.g. convective) terms together with a space discretization with spectral elements [16, 18] leads to

$$-\mathbf{D}\underline{V}^{n+1} = 0 \tag{29}$$

$$\left(\frac{\beta_{s_i}}{\Delta t}\right)\mathbf{M}\underline{V}^{n+1} - \mathbf{D}^{\mathrm{T}}\underline{P}^{n+1} + R_\mu \mathbf{K}\underline{V}^{n+1} + \mathbf{VE}\underline{T}^{n+1} = \frac{1}{\Delta t}\sum_{q=1}^{s_i}\beta_{s_i-q}\mathbf{M}\underline{V}^{n+1-q} - \sum_{r=0}^{s_e-1}\alpha_r\, Re\,\mathbf{C}(\underline{V}^{n-r}) \tag{30}$$

$$\left(\frac{We}{Re\,\Delta t}\beta_{s_i} + 1\right)\mathbf{M}\underline{T}^{n+1} = \frac{We}{Re\Delta t}\sum_{q=1}^{s_i}\beta_{s_i-q}\mathbf{M}\underline{T}^{n+1-q} + \sum_{r=0}^{s_e-1}\alpha_r\mathbf{NL}(\underline{T}^{n-r}, \underline{V}^{n-r}) \tag{31}$$

where an extrapolation method of order s_e has been used to determine the value of the non-linear term at time step $n+1$. The associated BDF scheme is of order s_i. The coefficients α_i and β_j are dependent of the orders of each method, e.g. for a BDF2/EX2 ($s_i = 2$, $s_e = 2$) scheme: $\alpha_0 = 2$, $\alpha_1 = -1$, $\beta_0 = -\frac{1}{2}$, $\beta_1 = 2$, $\beta_2 = \frac{3}{2}$. We have introduced a shorthand notation where $\underline{V}$, $\underline{P}$ and $\underline{T}$ represent the full vectors of all velocity, pressure and viscoelastic stress perturbation unknowns. The block diagonal matrices $\mathbf{M}$ and $\mathbf{K}$ are, respectively, composed with d block matrices M and K where d is the dimension of the problem. The matrix $\mathbf{D}$ corresponds to the full divergence operator and $\mathbf{D}^{\mathrm{T}}$ to the full gradient operator. The terms labelled with the symbols $\mathbf{C}$, $\mathbf{VE}$ and $\mathbf{NL}$ correspond to the convection of velocity, the divergence of the viscoelastic stress tensor and the non-linear terms in the constitutive equation.

An estimate of the leading eigenpairs of the linearized problem can be obtained after applying the operator C_T a large number of times on some initial vector X^0. After a certain number of applications i.e. at some time T_l, the resulting vector will contain only the effects of the leading eigenvectors after getting rid of the influence of the most quickly decaying eigenvectors. At this stage, m additional time steps or operator applications are carried out in order to generate vectors $X^{(1)} = X(T_l + \Delta t), \ldots, X^{(m)} = X(T_l + m\Delta t)$. This set of vectors can be processed with the Arnoldi method described previously in order to generate a set of

orthonormal vectors V_j $(1 \leqslant j \leqslant m)$ and therefore a matrix $\mathbf{H}^{(m)}$ from which approximations of the leading eigenpairs can be obtained after diagonalization. The eigenvalues Υ of the matrix $\mathbf{H}^{(m)}$ and those v of combined operators $\mathscr{B}$ and $\mathscr{A}$ in Equation (27) are related by $v \approx \mathrm{e}^{\Upsilon \Delta t}$.

An efficient alternative is to apply the Arnoldi method to the modified problem

$$X^{n+1} = (C_T - \Upsilon_s I)^{-1} X^n \tag{32}$$

or equivalently

$$(C_T - \Upsilon_s I) X^{n+1} = X^n \tag{33}$$

where I is the identity operator. The corresponding eigenvalues σ can be easily related to those of the original formulation Equation (27): $v \approx \mathrm{e}^{(1/\sigma + \Upsilon_s)\Delta t}$. The quantity Υ_s is a given real or complex number in the vicinity of which eigenvalues are searched for. The advantage of this approach over the previous one is that convergence towards eigenvalues close to Υ_s is faster, thus enabling the part of the spectrum close to Υ_s to be determined. Taking the inverse of operator $C_T - \Upsilon_s I$ enables us to get rid of dominant eigenvalues i.e. with large moduli. If Υ_s is complex, Equation (33) must be decomposed into its real and imaginary parts:

$$\begin{aligned} (C_T - (\Upsilon_s)_r I) X_r^{n+1} + (\Upsilon_s)_i X_i^{n+1} &= X_r^n \\ (C_T - (\Upsilon_s)_r I) X_i^{n+1} - (\Upsilon_s)_r X_r^{n+1} &= X_i^n \end{aligned} \tag{34}$$

Applying the operator C_T is Equation (33) is equivalent to proceeding one step of time integration backwards.

Let us emphasize that computing the quantity $C_T X^{n+1}$ is actually carried out by ultimately solving a system of the type $\mathbf{E}Y = \mathbf{F}$ to which a conjugate gradient method is applied. No explicit costly construction of the matrix E is required due to the efficient implementation of the tensor-product factorization involved in the spectral element method [35].

3.2. Results

Actually, the process described in the previous section is embedded in the IRAM algorithm. We will not give a presentation of this method here and refer the reader to relevant papers e.g. References [20, 22, 36]. We have implemented the technique described previously with success for simple test cases like the Couette and Poiseuille flows of viscoelastic fluids (see Figures 1 and 2). The linear stability of these flows has been studied theoretically by various authors e.g. [13, 17] and in particular by Wilson *et al.* [12] for Oldroyd-B fluids. Two groups of eigenvalues with real parts, respectively, equal to $-1/We$ and $-1/R_\mu We$ can be clearly identified and has also been reproduced numerically with a spectral element discretization [15, 16].

Examples of eigenvalues computed with the IRAM technique are given in Figures 3 and 4, respectively, for the Poiseuille and Couette flows of Oldroyd-B fluid ($R_\mu = 0.25$). Eigenvalues determined with a QZ algorithm used to compute the spectra presented in References [15, 16] related to the generalized eigenvalue problem described in Section 2 (Equation (18)) and for which the matrices A_h and B_h were explicitly built, have also been displayed as a reference. The matrix size of the corresponding eigenvalue problem is 218×218 for a crude mesh with one element (polynomial orders equal to $N_x = 4$ and $N_y = 7$, respectively, in the streamwise and cross-stream directions). Filled black delta and grey gradient triangles correspond to

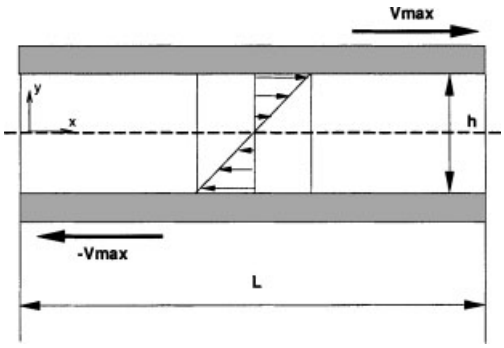

Figure 1. Couette flow in a planar channel.

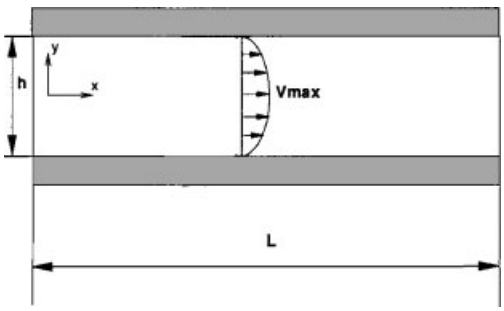

Figure 2. Poiseuille flow in a planar channel.

computations with the IRAM-based technique when the respective number of eigenvalues has been, respectively, fixed to 10 and 25 whereas empty squares are related to the QZ algorithm. Four complex shifts have been introduced for each problem. They have been selected so that their real parts are equal to either $-1/We$ or $-1/R_{\mu}We$ in order to be able to check that eigenvalues in the two characteristic sets could be accurately determined with the IRAM method. It can be seen on plots for both Poiseuille and Couette flows in Figures 3 and 4 showing the computed local spectra for the two numbers of eigenvalues ($m = 10$ and 25) that accurate results have been obtained with this algorithm provided that a small set of eigenvalues is used (typically $m = 10$ is sufficient). It is therefore not necessary to retain more modes in the computations.

3.3. Extension to complex flows

This method could be applied in the future to determine in particular the most dangerous eigenvalues of complex viscoelastic (and clearly also Newtonian) flows and would therefore provide a useful tool to address BiGlobal and possibly TriGlobal instabilities [37].

In a recent paper, Smith *et al.* [7] have presented such numerical methods based on finite elements for the analysis of the stability of two-dimensional steady viscoelastic flows

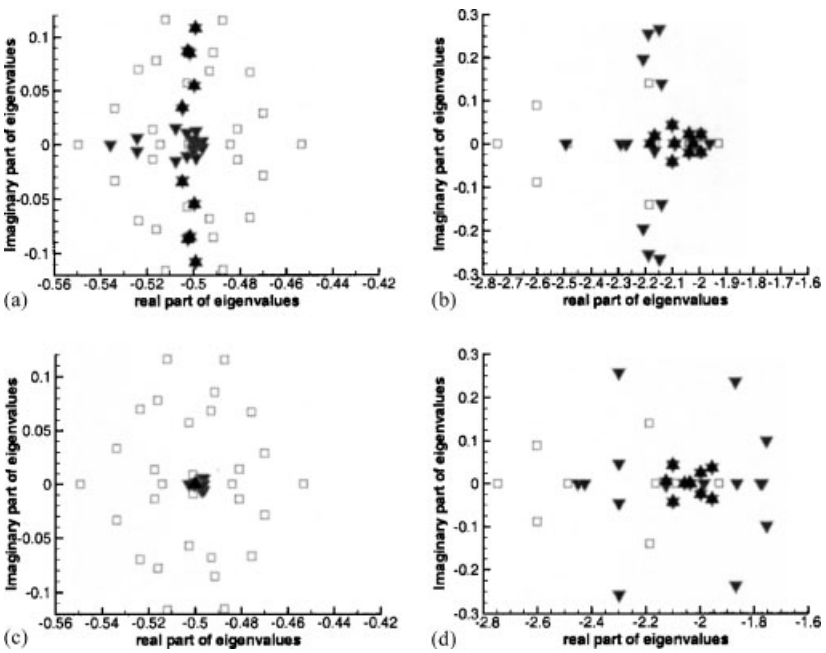

Figure 3. Part of the eigenvalue spectra for the Poiseuille flow of an Oldroyd-B fluid ($We = 2.0$, $R_\mu = 0.25$, 1 element $N_x = 4$, $N_y = 7$). Filled black delta and grey gradient triangles correspond to eigenvalues computed with the IRAM-based technique with, respectively, 10 and 25 retained eigenvalues. Empty square symbols are relative to the data computed with the QZ algorithm. Complex shifts equal to: $-0.5 + i0.1$ (a), $-2.0 + i0.1$ (b), $-0.5 + i0.001$ (c), $-2.0 + i0.001$ (d).

to small amplitude, two-dimensional and three-dimensional disturbances. In order to reduce the problem size, they restricted their study to viscoelastic stress perturbations. They tested two different time integration schemes to compute the evolution of disturbances: a θ-method operator splitting technique [19] and a fourth-order Runge–Kutta method. As for as the stability of the spacial discretization is concerned, both SUPG and DG techniques have been used in addition to the standard Galerkin method. Although they resorted to an implicit technique to compute the steady-state solutions, time-dependent simulations have been carried out by decoupling the full problem into a modified Stokes problem and an evaluation of the constitutive equation, which is basically the type of technique that we have used in our simulations [16, 18]. Smith *et al.* applied the IRAM method [21] mentioned previously.

They validated their formulation by applying it to the circular Couette flow of an Oldroyd-B fluid for which a well-documented list of transitions to three-dimensional time-periodic state occurring at given values of the Weissenberg number has been established e.g. [38]. In addition, they underlined the dissipative effects of the SUPG method, which strongly modifies the eigenvalue spectrum compared to the one computed with a classical Chebyshev method. Modes were not only shifted but could also disappear. Classical Galerkin (when stable) and DG techniques provided significantly better results.

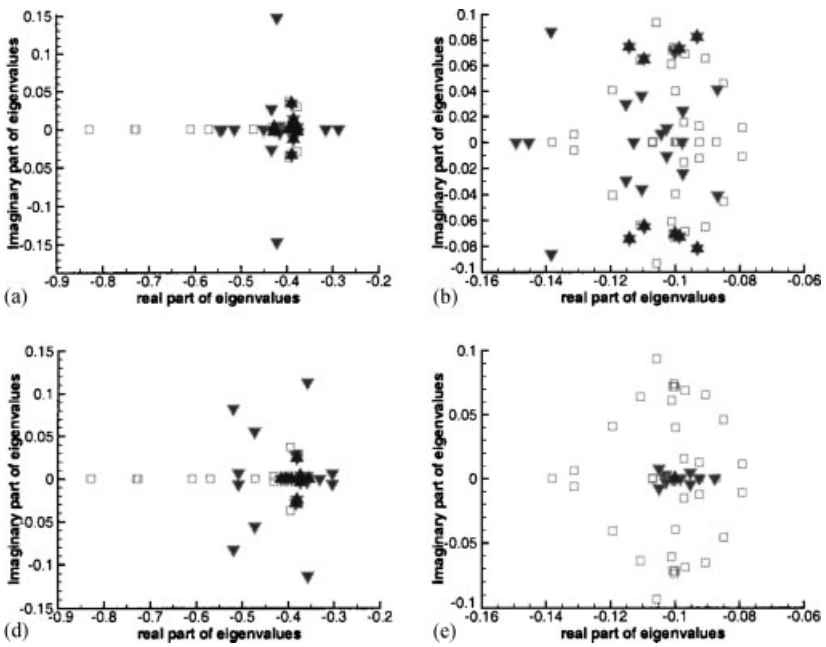

Figure 4. Part of the eigenvalue spectra for the Couette flow of an Oldroyd-B fluid ($We = 10.0$, $R_\mu = 0.25$, 1 element $N_x = 4$, $N_y = 7$). Filled black delta and grey gradient triangles correspond to eigenvalues computed with the IRAM-based technique with, respectively, 10 and 25 retained eigenvalues. Empty square symbols relate to the data computed with the QZ algorithm. Complex shifts equal to: $-0.4 + i0.1$ (a), $-0.1 + i0.1$ (b), $-0.4 + i0.001$ (c), $-0.1 + i0.001$ (d).

In a second step, the method was applied to the stability of the flow around a closely spaced linear array of cylinders. It was emphasized that under-resolution of the continuous spectrum lead to treacherous numerical time-periodic instabilities that were apparently convergent when direct time integration was used. The Arnoldi-based method enabled the authors to diagnose that the dominant mode on a given mesh became stable and was superseded by a new dominant mode with a higher wave number when the mesh was refined. In contrast to the circular Couette flow, for which the discrepancies between the modes computed with the SUPG and DG methods were reduced with mesh refinement, the temporal or spatial structure of disturbances obtained with the two discretizations never matched no matter how refined the mesh was. This emphasizes the fact that the structure of the long-time perturbation is very sensitive to spatial discretization. The flow was found stable if the mesh was properly refined for the range of investigated Weissenberg numbers ($We \leqslant 1.5$) with both methods.

They also considered the stability of the flow of an Oldroyd-B fluid around a confined cylinder when submitted to three-dimensional perturbations. The same problem has been studied experimentally by McKinley *et al.* [39]. As opposed to experimental results, no transition from the two-dimensional base flow to a three-dimensional cellular structure in the cylinder wake has been detected numerically in the range of investigation ($We \leqslant 0.75$). The reason for this discrepancy is not clear. However, it is suspected that the steady-state stress distribution in the

flow obtained with a single-mode Oldroyd-B model is quite different from the experimental case. Subsequently, a more sophisticated constitutive model would be required to establish a more relevant comparison with experiments. Whether the Oldroyd-B constitutive equation is able to reproduce flow transitions in complex flows is still an open question. The range of investigation has only been restricted by numerical limitations due to the impossibility of solving properly the steady-state flow at higher Weissenberg numbers. If this upper limit could be extended, flow transition might appear with an Oldroyd-B fluid at higher values of *We*.

The work of Smith *et al.* emphasizes the difficulty of detecting physical instabilities with numerical simulations of complex viscoelastic flows and the need for complementary techniques based on stability analysis to investigate the possible evidence of numerically induced instabilities.

4. TRANSIENT GROWTH OF PERTURBATIONS

Following investigations of possible linear mechanisms related to the transient growth of infinitesimal perturbations for the induction of transition between laminar and turbulent regimes in Newtonian shear flows e.g. References [23, 24], the influence of the non-normality of the linearized differential operators present in the equations describing the flow of viscoelastic fluids has been recently studied e.g. References [19, 25]. Non-normality of the eigenvectors is a consequence of the non-commutability of the linearized differential operators with their adjoints as shown e.g. in References [23, 25], and results in transient growth if disturbances become perpendicular to the eigenvectors (misfit disturbances). If the amplitude growth is large enough, non-linear effects come into play possibly leading to further recreation of misfit disturbances in a positive feedback process.

Based on the analysis of Grossmann [23] for Newtonian fluids, Atalık and Keunings [25] have provided a simplified theory of possible non-normality effects due to the terms related to the advection and deformation of the base Couette flow of a UCM or Oldroyd-B fluid by the perturbation as *We* increases: $Re(\mathbf{v}_1 \cdot \nabla)\mathbf{v}_0$ in Equation (6) and $We[(\mathbf{v}_1 \cdot \nabla)\boldsymbol{\tau}_0 - \boldsymbol{\tau}_1 \cdot (\nabla \mathbf{v}_0)^{\mathrm{T}} - \nabla \mathbf{v}_1 \cdot \boldsymbol{\tau}_0]$ in Equation (7). Although they did not mention it explicitly, the convective term $(\mathbf{v}_1 \cdot \nabla)\boldsymbol{\tau}_0$ in the constitutive equation vanishes because the steady-state viscoelastic stress tensor does not vary spatially for the Couette flow of such fluids. The terms concerned with the advection and deformation of the perturbation fields by the base flow do not determine the growth or decay of the perturbations since they are globally energy conserving.

We have noticed by carrying out numerical simulations of these benchmark problems with the non-linearized conservation and constitutive equations that the instabilities were generated either by the convective terms or the terms involving the velocity gradients in the constitutive equation by systematically replacing each term in turn by its analytical steady-state expression thus suppressing its effect on the perturbation. Although numerical instabilities are first driven by the convective term, they may also arise even if it is prescribed through the velocity gradient terms in agreement with the analysis of Atalık and Keunings.

Simulations using linearized equations have also been performed in order to check that similar results were obtained for small amplitude perturbations (typically of the order of 10^{-3} times the steady-state reference value). Above that level non-linear effects could be observed in agreement with the findings of Sureshkumar *et al.* [19] for the Couette flow of UCM and Oldroyd-B fluids and for the flow of an Oldroyd-B fluid past an array of

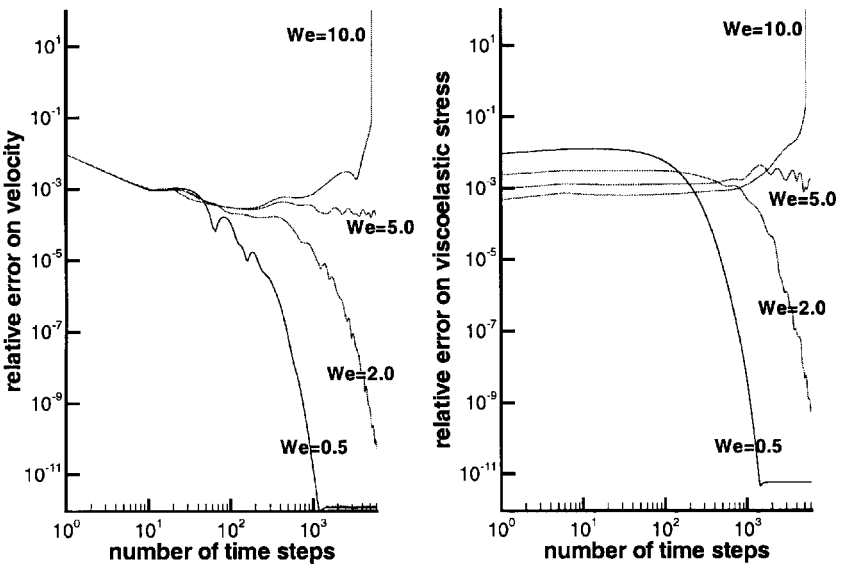

Figure 5. Temporal variations of the relative error on the velocity $\|\mathbf{v} - \mathbf{v}_{\text{analytical}}\|_E / \|\mathbf{v}_{\text{analytical}}\|_E$ (left) and on the viscoelastic stress tensor $\|\tau - \tau_{\text{analytical}}\|_E / \|\tau_{\text{analytical}}\|_E$ for the Poiseuille flow of an Oldroyd-B fluid (Euclidian norms).

cylinders. The influence of transient growth on the numerical stability of our simulations as the Weissenberg number increases can be readily observed in Figure 5 for a Poiseuille flow of an Oldroyd-B fluid ($R_\mu = 0.25$, time step $\Delta t = 0.01$). A single element was used for the discretization with polynomial orders equal to $N_x = 4$ in the streamwise direction and $N_y = 7$ in the cross-stream direction. At low Weissenberg numbers, the decay of the perturbation after some short period can be observed. The action of several modes through non-normality and subsequent non-linear effects can then be identified as We increases after some time. The left and right plots, respectively, correspond to relative errors of the velocity and viscoelastic stress based on Euclidian norms. Analytical expressions of these quantities can be easily obtained for the steady Poiseuille flows of Oldroyd-B fluids [16].

To demonstrate non-normality among the eigenvectors, Figure 6 shows a typical matrix filled with the values of some debunching (as opposed to overlap) function of the normalized eigenvectors corresponding to the most dangerous eigenvalues for the Poiseuille flow of an Oldroyd-B fluid for $We = 2.0$. By debunching, we mean that no large bunches of eigenvectors are pointing into specific mean directions. A single element was used for the discretization with polynomial orders equal to $N_x = 4$ in the streamwise direction and $N_y = 7$ in the cross-stream direction. Cell (i, j) corresponds to the value of the debunching function $f(X_i, X_j) = 1 - \frac{1}{2}(X_i \cdot X_j^* + X_j \cdot X_i^*)$ of the ith and jth eigenvectors X_i and X_j, where X^* denotes the complex conjugate of X. Eigenvalues are ordered according to decreasing real parts. Darker cells correspond to larger overlap of eigenvectors. If all eigenvectors were orthogonal, only the cells on the diagonal would be black. White cells indicate that the eigenvectors are orthogonal. It can be seen that non-normality of the eigenvectors does induce some overlap or bunching

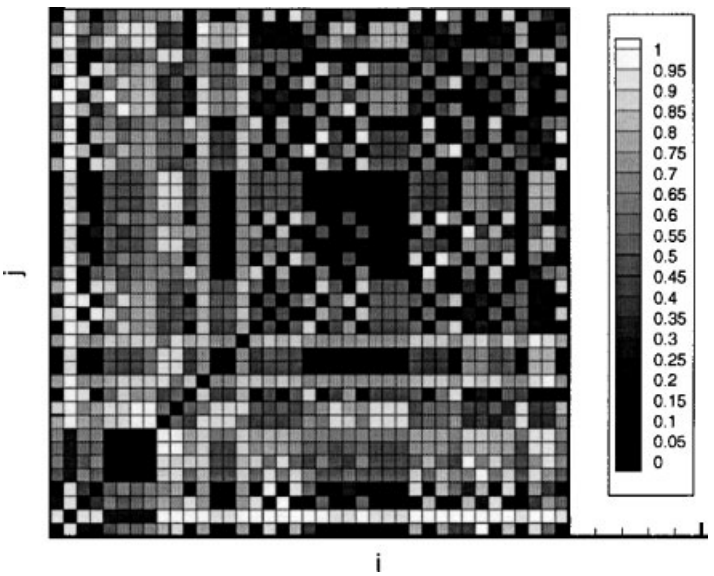

Figure 6. Matrix of the debunching function $f(X_i, X_j)$ of the normalized eigenvectors corresponding to the most dangerous eigenvalues for the Poiseuille flow of an Oldroyd-B fluid ($N_x = 4$, $N_y = 7$, $L/h = 8$, $R_\mu = 0.25$, $We = 2.0$) (see text for the definition of f).

among the eigenvectors. This effect is even stronger for larger values of We as expected. This is visible in Figure 7 for $We = 10.0$ where a large amount of overlap can be observed between the eigenvectors (low values of the debunching function).

5. CONCLUSION

Being able to investigate instabilities numerically is one of the most challenging topic in the field of viscoelastic flow research. In particular, one must be able to distinguish between true physical and numerically induced instabilities which may appear in simulations. To this end, it is necessary to develop tools that would enable one to diagnose the type and characteristics of detected perturbations in the flows. This paper points out to such a method, which enables one to proceed to such investigation. Thus, the implementation of a technique based on Arnoldi's method to determine the leading eigenvalues relative to complex flows has been presented.

Tracking such instabilities requires the use of accurate techniques. As far as the spatial discretization is concerned, the most popular methods have been by far based on finite volumes and finite elements. Recently, alternative techniques based on Legendre spectral element methods have been applied with success to simulate viscoelastic flows e.g. References [18, 29, 30]. They combine the ability to treat complicated geometries like the classical (low-order) finite-element methods with the accuracy of high-order approximation polynomials encountered in spectral methods.

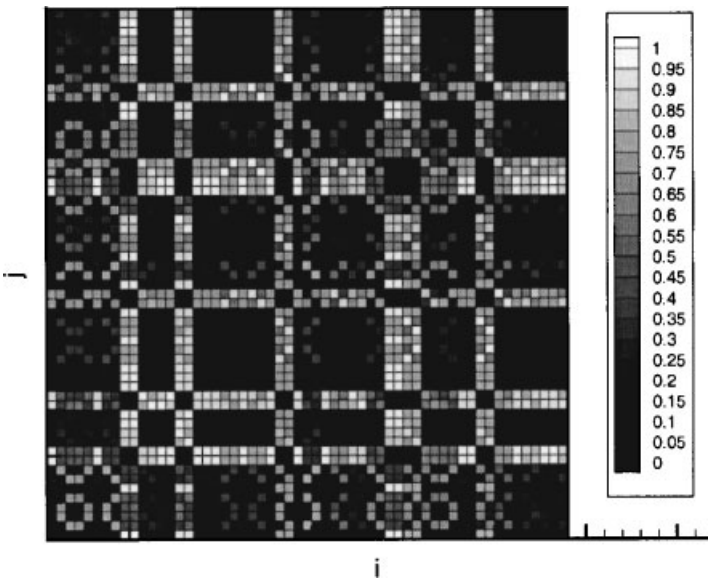

Figure 7. Matrix of the debunching function $f(X_i, X_j)$ of the normalized eigenvectors corresponding to the most dangerous eigenvalues for the Poiseuille flow of an Oldroyd-B fluid ($N_x = 4$, $N_y = 7$, $L/h = 64$, $R_\mu = 0.25$, $We = 10.0$) (see text for the definition of f).

The proposed method benefits from the fact that no implicit construction of the matrices appearing in matrix–vector products is required as ensured by the tensor-product factorization inherent in efficient algorithms using spectral elements for the spatial discretization. Although we have only tested it on simple problems, it will be applied to large-scale problems like e.g. the flow through a contraction in the future.

Following a study of the onset of numerical instabilities in simulations of viscoelastic flows, effects of transient growth due to non-normality of the operators involved in the conservation and constitutive equations have been shown to be a potential source of numerical instability fostered by the discretization.

ACKNOWLEDGEMENTS

The author is thankful to Dr V. Theofilis ad Dr L.S. Tuckermann for pointing out the potential of Arnoldi methods to solve generalized eigenvalue problems and to Prof. M.O. Deville for promoting this study and proof-reading this manuscript. This research has been partially funded by a Swiss National Science Foundation grant (No. 20-59357.99), whose support is gratefully acknowledged.

REFERENCES

1. Bodardt C. Ecoulements viscoélastiques transitoires et sédimentation. *Ph.D. Thesis*, Département de Mécanique, Université catholique de Louvain, Louvain-la-Neuve, Belgium, 1994.
2. Larson RG. Instabilities in viscoelastic flows. *Rheologica Acta* 1992; **31**:213–263.
3. McKinley GH, Pakdel P, Öztekin A. Rheological and geometric scaling of purely elastic flow instabilities. *Journal of Non-Newtonian Fluid Mechanics* 1996; **67**:19–47.

4. Petrie CJS, Denn MM. Instabilities in polymer processing. *A.I.C.h.E. Journal* 1976; **22**:209–236.
5. Shaqfeh ESG. Purely elastic instabilities in viscometric flows. *Annual Review of Fluid Mechanics* 1996; **28**: 129–185.
6. Tanner RI. *Engineering Rheology*. Oxford University Press: Oxford, 1988.
7. Smith MD, Armstrong RC, Brown RA, Sureshkumar R. Finite element analysis of stability of two-dimensional viscoelastic flows to three-dimensional perturbations. *Journal of Non-Newtonian Fluid Mechanics* 2000; **93**: 203–244.
8. Drazin PG, Reid WH. *Hydrodynamic Instability*. Cambridge University Press: New York, 1981.
9. Guckenheimer J, Holmes P. *Nonlinear Oscillations, Dynamical Systems, and Bifurcations of Vector Fields*, Applied Mathematical Sciences, vol. 42. Springer: New York, 1983.
10. Iooss G, Joseph DD. *Elementary Stability and Bifurcation Theory*. Springer: New York, 1990.
11. Schmid PJ, Henningson DS. *Stability and Transition in Shear Flows*. Applied Mathematics and Science, vol. 142. Springer: New York, 2001.
12. Wilson HJ, Renardy M, Renardy Y. Structure of the spectrum in zero Reynolds number shear flow of the UCM and Oldroyd-B liquids. *Journal of Non-Newtonian Fluid Mechanics* 1999; **80**:251–268.
13. Grillet AM, Bogaerds ACB, Peters GWM, Baaijens FPT. Stability analysis of constitutive equations for polymer melts in viscometric flows. *Journal of Non-Newtonian Fluid Mechanics* 2002; **103**:221–250.
14. Fiétier N, Deville MO. Time-dependent algorithms for the simulation of viscoelastic flows with spectral element methods: applications and stability. *Journal of Computational Physics* 2003; **186**:93–121.
15. Fiétier N, Deville MO. Linear stability analysis of time-dependent algorithms with spectral element methods for the simulation of viscoelastic flows. *Journal of Non-Newtonian Fluid Mechanics* at press.
16. Fiétier N. Numerical simulation of viscoelastic fluid flows by spectral element methods and time-dependent algorithms. *Ph.D. Thesis*, No. 2631, Department of Mechanical Engineering, Swiss Federal Institute of Technology, Lausanne, 2002.
17. Renardy M, Renardy Y. Linear stability of plane Couette flow of an upper convected Maxwell fluid. *Journal of Non-Newtonian Fluid Mechanics* 1986; **22**:23–33.
18. Fiétier N, Deville MO. Simulations of time-dependent flows of viscoelastic fluids with spectral element methods. *Journal of Scientific Computing* 2002; **17**:649–657.
19. Sureshkumar R, Smith MD, Armstrong RC, Brown RA. Linear stability and dynamics of viscoelastic flows using time-dependent numerical simulations. *Journal of Non-Newtonian Fluid* 1999; **82**:57–104.
20. Lehoucq RB, Sorensen DC. Deflation techniques for an implicitly re-started Arnoldi iteration. *SIAM Journal on Matrix Analysis and Applications* 1996; **17**:789–821.
21. Lehoucq RB, Sorensen DC, Yang C. *ARPACK's User's Guide*: *Solution of Large-Scale Eigenvalue Problems with Implicitly Restarted Arnoldi Methods*. http:/www.caam.rice.edu/software/ARPACK [10 October 2001].
22. Edwards WS, Tuckerman LS, Friesner RA, Sorensen DC. Krylov methods for the incompressible Navier–Stokes equations. *Journal of Computational Physics* 1994; **110**:82–102.
23. Grossmann S. The onset of shear flow turbulence. *Reviews of Modern Physics* 2002; **72**:603–618.
24. Trefethen LN, Trefethen AE, Reddy SC, Driscoll TA. Hydrodynamic instability without eigenvalues. *Science* 1993; **261**:578–584.
25. Atalık K, Keunings R. Non-linear temporal stability analysis of viscoelastic plane channel flows using a fully-spectral method. *Journal of Non-Newtonian Fluid Mechanics* 2002; **202**:299–319.
26. Leriche E. Direct numerical simulation of a lid-driven cavity flow by a Chebyshev spectral method. *Ph.D. Thesis*, No. 1932, Department of Mechanical Engineering, Swiss Federal Institute of Technology, Lausanne, 1999.
27. Fischer PF. Parallel domain decomposition for incompressible fluid dynamics. *Contemporary Mathematics* 1994; **AMS 157**:313–322.
28. Fischer PF, Kruse GW, Loth F. Spectral element methods for transitional flows in complex geometries. *Journal of Scientific Computing* 2002; **17**:81–98.
29. Chauvière C, Owens RG. How accurate is your solution? Error indicators for viscoelastic flow calculations. *Journal of Non-Newtonian Fluid Mechanics* 2000; **95**:1–33.
30. Van Kemenade V, Deville MO. Application of spectral elements to viscoelastic creeping flows. *Journal of Non-Newtonian Fluid Mechanics* 1994; **51**:277–308.
31. Christodoulou KN, Scriven LE. Finding leading modes of a viscous free surface flow: an asymmetric generalized eigenproblem. *Journal of Scientific Computing* 1988; **3**:355–406.
32. Tuckerman LS, Bertagnolio F, Daube O, Le Quéré P, Barkley D. Stokes preconditioning for the inverse Arnoldi method. In *Continuation Methods in Fluid Dynamics*, Henry D, Bergeon A (eds). Vieweg: Wiesbaden, 2000; 241–255.
33. Tuckerman LS, Barkley D. Bifurcation analysis for time-steppers. In *Numerical Methods for Bifurcation Problems and Large-Scale Dynamical Systems*, Doedel E, Tuckerman LS (eds). Springer: Berlin, 1999; 453–466.
34. Saad Y, Schultz M. GMRES: A generalized minimal residual algorithm for solving nonsymmetric linear systems. *SIAM Journal on Scientific and Statistical Computing* 1986; **7**:856–869.

35. Deville MO, Fischer PF, Mund EH. *High-Order Methods for Incompressible Fluid Flow*. Cambridge University Press: New York, 2002.
36. Sorensen DC. Implicit application of polynomial filters in a k-step Arnoldi method. *SIAM Journal on Matrix Analysis and Applications* 1992; **13**:357–385.
37. Theofilis V. Advances in global linear instability analysis of non-parallel and three-dimensional flows. *Progress in Aerospace Sciences* 2003; **39**:249–315.
38. Avgousti M, Beris AN. Non-axisymmetric modes in viscoelastic Taylor–Couette flow. *Journal of Non-Newtonian Fluid Mechanics* 1993; **50**:225–251.
39. McKinley GH, Brown RA, Armstrong RC. The wake instability in viscoelastic flow past confined circular cylinders. *Philosophical Transactions of the Royal Society London Series A* 1993; **344**:265–304.

